Supporting Information

Precisely tailoring ZIF-67 Nanostructures from cobalt carbonate hydroxide nanowire arrays: toward high-performance battery-type electrodes

Dongbo Yu,[a]Liang Ge,[a] Bin Wu,[a] Liang Wu,[a] Huanting Wang [b] and Tongwen Xu [*, a]

[a] *CAS Key Laboratory of Soft Matter Chemistry, Collaborative Innovation Center of Chemistry for Energy Materials, School of Chemistry and Material Science, University of Science and Technology of China, Hefei 230026, People's Republic of China*

[b] *Department of Chemical Engineering, Monash University, Clayton, Victoria 3800, Australia*

E-mail addresses: twxu@ustc.edu.cn

Experimental Section

Synthesis of dense and less-dense cobalt carbonate hydroxide nanowire arrays on Ni foam

In a typical synthesis, Ni foam (3 cm*4 cm in rectangular shape) was placed in 3 M HCl solution with ultrasonic for 30 min to remove the surface oxide layer and washed with ethanol and water for several times. 5 mmol of $Co(NO_3)_2$, 10 mmol of NH_4F and 25 mmol of $CO(NH_2)_2$ were dissolved in 50 mL of distilled water. Subsequently, the resulting solution was transferred into a Teflon-lined stainless steel autoclave with a capacity of 65 ml and the Ni foam was immersed into the precursor solution. The top side of Ni foam was coated with a polytetrafluoroethylene tape to prevent the undesired deposition from the reaction. The autoclave was sealed and heated at 90 °C for 12 h, and then cooled to room temperature naturally. The pink-colored dense cobalt carbonate hydroxide nanowire array (Co-NWA) supported on Ni foam was obtained. Less-dense Co-NWA was synthesized through the similar method without adding NH_4F, because the presence of NH_4F enabled more favarable nucleaction of cobalt carbonate hydroxide nanocrystals in the formation of the nanowires.[1] In addition, the synthesis of cobalt carbonate hydroxide nanowire (Co-NW) powder followed the procedure of less-dense cobalt carbonate hydroxide nanowire array without using the Ni foam substrate.

Synthesis of ZIF-67-based nanostructures including bead-on-string structure, core-shell nanowire, nanotube and nanoflake

ZIF-67-based nanostuctures with various morphologies were achieved by carefully controlling the transformation parameters including reaction time, temperature and concentration of precursor solution. The as-prepared less-dense cobalt carbonate hydroxide nanowire array was directly immersed into 2-methylimidazole aqueous solution (5 g of 2-methylimidazole in 20 ml water) at room temperature for 16 h, bead-on-string structured ZIF67 particles@Co-NW nanowire array was synthesized. When 4 g of triethylamine (TEA) was introduced into the precursor solution and the reaction was placed at an electric oven at 75°C for 60 min, ZIF67@Co-NW core-shell nanowire array (ZIF-CSNWA) was obtained. Further prolonging the reaction time to

120 min, it generated ZIF67-based nanotube array (ZIF-NTA). And if a dense cobalt carbonate hydroxide nanowire array was used, ZIF-67-based nanoflake morphology was formed finally. The prepared ZIF-67-based nanostuctured materials were thoroughly washed with ethanol and water for more than 10 times to eliminate the possible 2-methylimidazole residues.

Synthesis of mesoporous Co_3O_4 nanotube array

ZIF-NTA was annealed at 350 °C in air for 2 h at the heating rate of 2°C/min to obtain mesoporous Co_3O_4 nanotube array (Co_3O_4-NTA). For comparison, directly Co-NWA-derived Co_3O_4 nanowire array (Co_3O_4-NWA) and ZIF-CSNWA-derived core-shell Co_3O_4 nanowire array (Co_3O_4-CSNWA) were also prepared by heating Co-NWA and ZIF-CSNWA, the annealing treatment was the same as Co_3O_4-NTA. The weight of Co_3O_4-NWA, Co_3O_4-CSNWA and Co_3O_4-NTA on Ni foam was measured by calculating the increased mass of Ni foam after reaction and heat treatment, and their mass loading was 4.1, 4.0 and 3.4 mg/cm^2, respectively.

Materials characterizations and electrochemical measurements

The X-ray diffraction (XRD) measurement was carried out on a Rigaku D/MAX2500VL/PC X-ray diffractometer with Cu K_α radiation. The morphology of the composite was determined by field-emission scanning electron microscopy (SEM, SU8020) and a transmission electron microscopy (TEM, JEM-2100) operated at 200 KV. The samples were analyzed by the nitrogen sorption technique using a Micromeritics ASAP 2020 instrument at 77 K, and their surface area was calculated by using the Brunauer-Emmett-Teller (BET) method in the relative pressure (P/P_o) range of 0.002-0.3. Thermal gravity analysis (TGA) was conducted on a simultaneous thermal analyzer (STA, STA449F3) from room temperature to 800 °C at the heating rate of 10 °C/min. The electrochemical performance was investigated by cyclic voltammetry (CV), electrochemical impedance spectroscopy (EIS) and galvanostatic charge-discharge in 2 M KOH solution using an electrochemical workstation (Autolab 3). The nickel foam supported electroactive materials (~ 4 cm^2 in area) were directly used as the working electrode. The KCl saturated Ag/AgCl and

Pt rod were used as the reference electrode and the counter electrode respectively. EIS measurements were tested in the frequency range from 0.1Hz to 100 kHz at open-circuit potential with an ac perturbation of 0.1 V. The area capacity (C/cm^2) of the electrodes was calculated based on Equation 1 (CV plots) and Equation 2 (galvanostatic charge/discharge curves), and the specific capacity of the electrode was calculated by Equation 3:

$$C_a = \frac{\int_{Va}^{Vc} I(V)dV}{S\nu} \qquad \text{Equation 1}$$

Where C_a is the area capacity (C/cm^2), S is the geometrical area of the electrode (cm^2), ν is the scan rate of CV curves (V/s).

$$C_a = \frac{I\Delta t}{S} \qquad \text{Equation 2}$$

Where C_a is the area capacity (C/cm^2), I is the discharge current (A), S is the geometrical area of the electrode (cm^2) and Δt is the total discharge time (s).

$$C_s = \frac{I\Delta t}{m} \qquad \text{Equation 3}$$

Where C_s is the specific capacity (C/g), I is the discharge current (A), m is the mass of the active materials (g) and Δt is the total discharge time (s).

1 J. Jiang, J. P. Liu, X. T. Huang, Y. Y. Li, R. M. Ding, X. X. Ji, Y. Y. Hu, Q. B. Chi and Z. H. Zhu, *Cryst. Growth Des.*, 2010, **10**, 70-75.

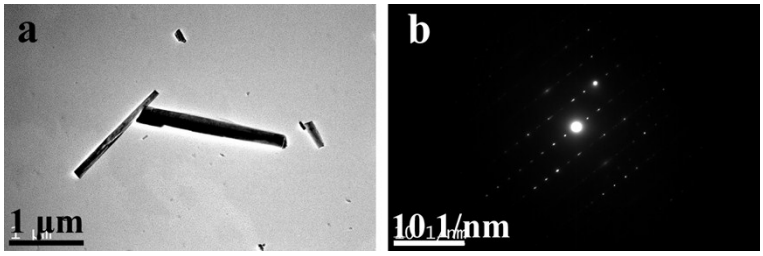

Figure S1 TEM images of $Co(CO_3)_{0.5}(OH)\cdot 0.11H_2O$ nanowires (a) and the corresponding electron diffraction pattern (b). The electron diffraction spots indicated the single-crystal structure of $Co(CO_3)_{0.5}(OH)\cdot 0.11H_2O$ nanowires.

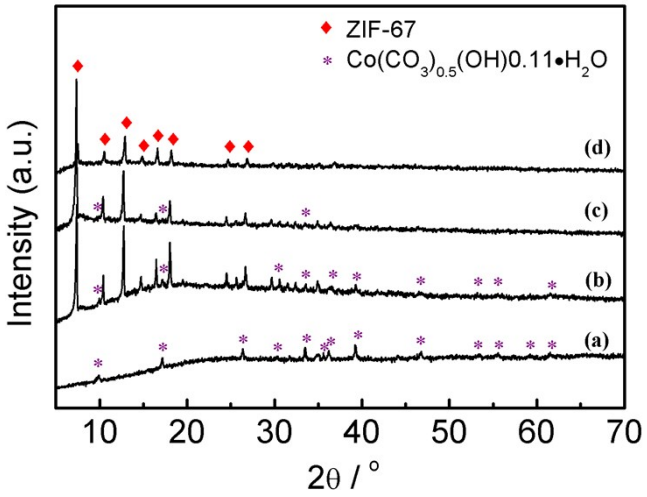

Figure S2 XRD patterns of $Co(CO_3)_{0.5}(OH)\cdot 0.11H_2O$ nanowires (a) and resulting materials in aqueous solution at room temperature after different reaction time of 24 h (b), 7 days (c) and 7 days in addition of TEA (d).

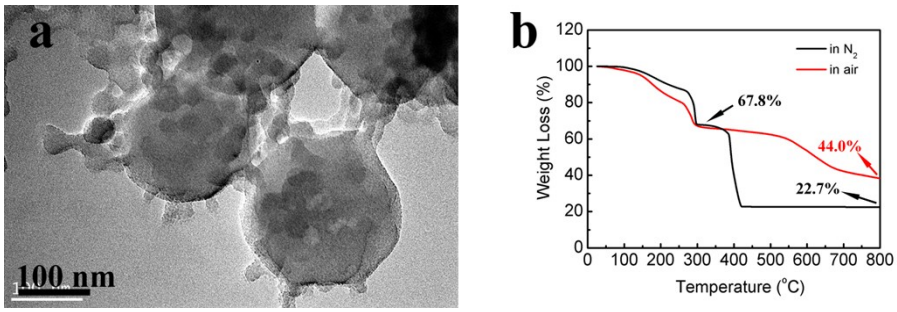

Figure S3 TEM image (a) and TGA results (b) of ZIF67 (7-day reaction in addition with TEA).

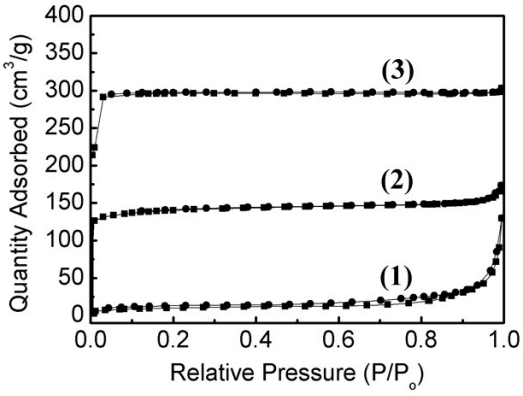

Figure S4 Nitrogen adsorption–desorption isotherms of resulting materials in aqueous solution at room temperature after different reaction time of 24 h (1), 7 days (2) and 7 days in addition of TEA (3).

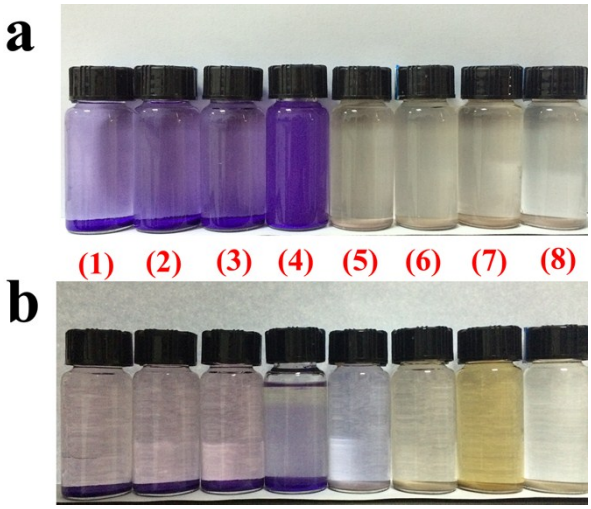

Figure S5 Optical images of the conversion of $Co(CO_3)_{0.5}(OH)\cdot 0.11H_2O$ nanowire powder into ZIF-67 at room temperature (a) and 75°C (b) by varying the reaction parameters: in water for 24 h (1), in water for 48 h (2), in water for 7 days (3), in water + TEA for 7 days (4), in ethanol for 7 days (5), in methanol for 7 days (6), in NMP for 7 days (7), in DMF for 7 days (8). From the images, only when in water did the color of $Co(CO_3)_{0.5}(OH)\cdot 0.11H_2O$ nanowires turn into violet of ZIF-67 from pink. In later experiments, we realized that even though the temperature was increased to 100°C and the reaction time lasted for half of month, the powders in ethanol, methanol, NMP and DMF didn't change the color, indicating the kinetics of transformation was more likely to depend on the applied solvent rather than the temperature.

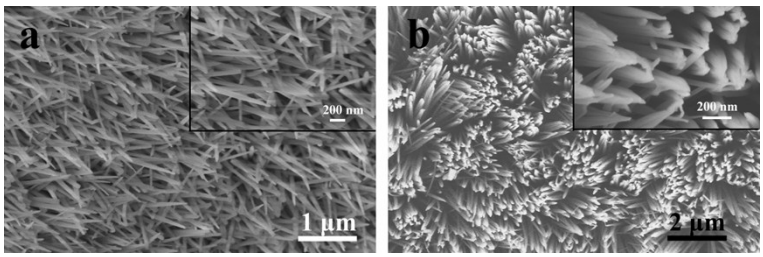

Figure S6 SEM images of the precursor $Co(CO_3)_{0.5}(OH)\cdot 0.11H_2O$ nanowire array: less-dense (a) and dense (b)

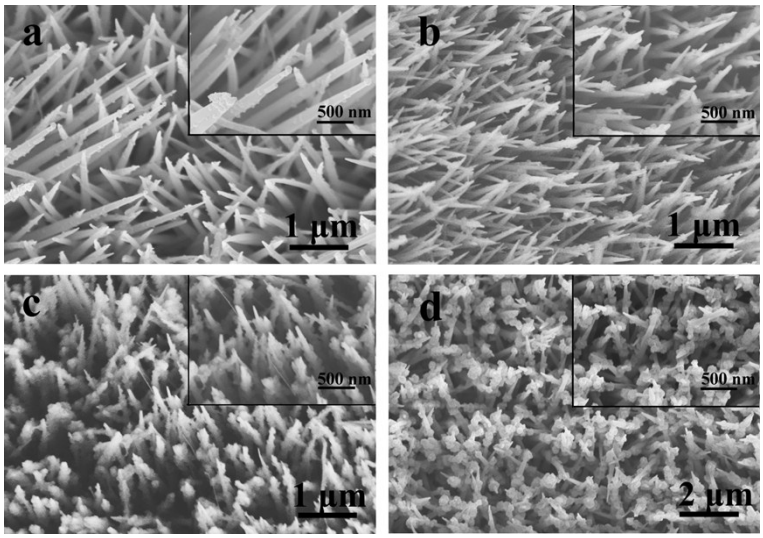

Figure S7 SEM images of less-dense $Co(CO_3)_{0.5}(OH)\cdot 0.11H_2O$ nanowire array in high-concentration solution (5 g of 2-methylimidazole in 20 ml water) at room temperature for 4 h (a), 8 h (b), 12 h (c) and 16 h (d).

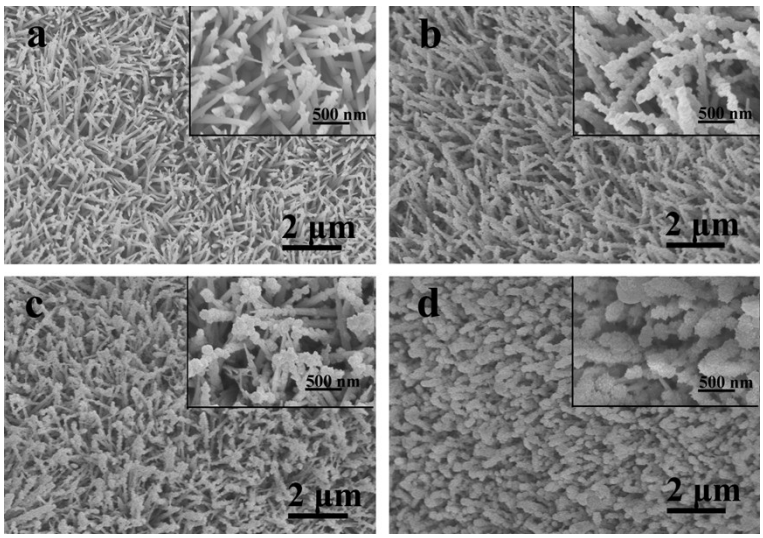

Figure S8 SEM images of less-dense $Co(CO_3)_{0.5}(OH)\cdot 0.11H_2O$ nanowire array in high-concentration solution at 50°C for 45 min (a), 90 min (b), 135 min (c) and 180 min (d).

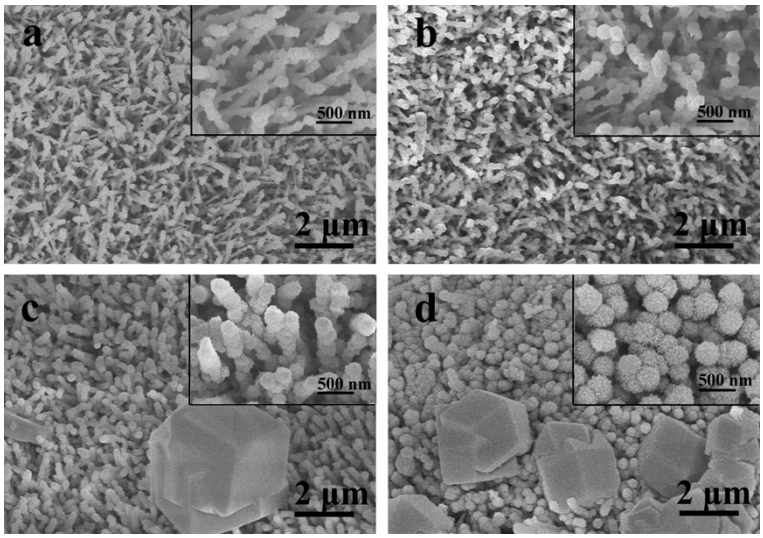

Figure S9 SEM images of less-dense $Co(CO_3)_{0.5}(OH)\cdot 0.11H_2O$ nanowire array in high-concentration solution at 75°C for 30 min (a), 60 min (b), 90 min (c) and 120 min (d).

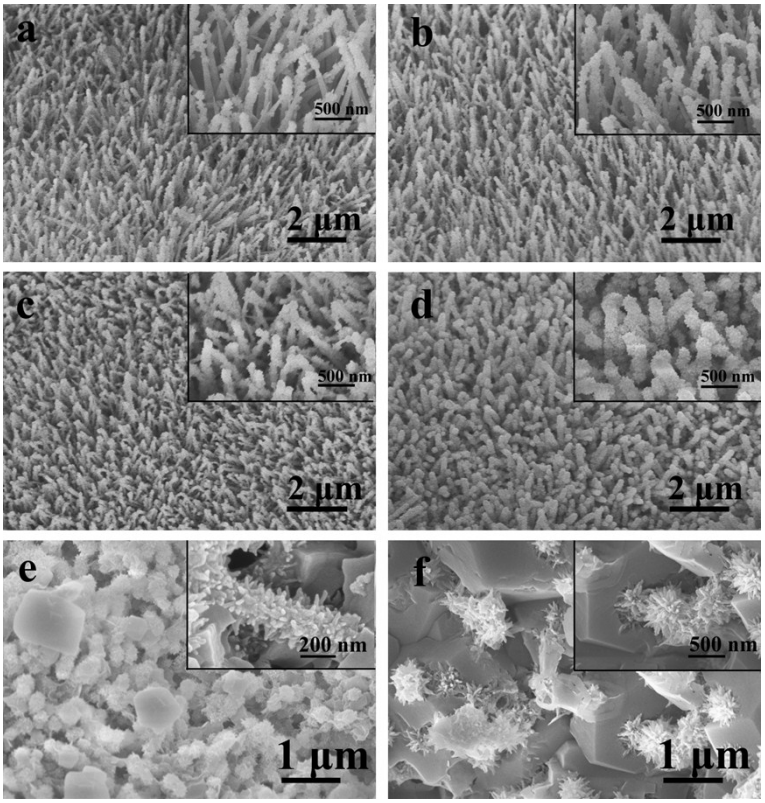

Figure S10 SEM images of less-dense $Co(CO_3)_{0.5}(OH)\cdot 0.11H_2O$ nanowire array in low-concentration solution (2.5 g of 2-methylimidazole in 20 ml water) at 75°C for 60 min (a), 120 min (b), 180 min (c), 240 min (d), 300 min (e) and 360 min (f).

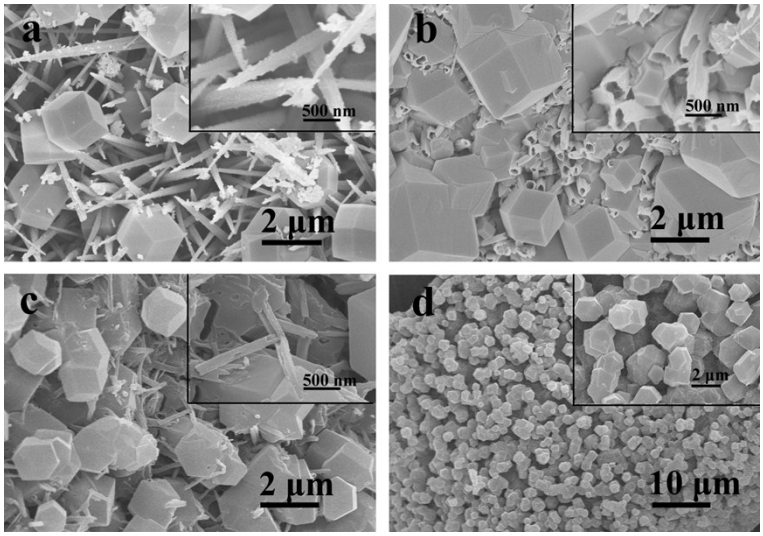

Figure S11 SEM images of less-dense $Co(CO_3)_{0.5}(OH)\cdot 0.11H_2O$ nanowire array in addition of triethylamine at 75°C for 60 min (a), 120 min (b), 180 min (c) and 240 min (d).

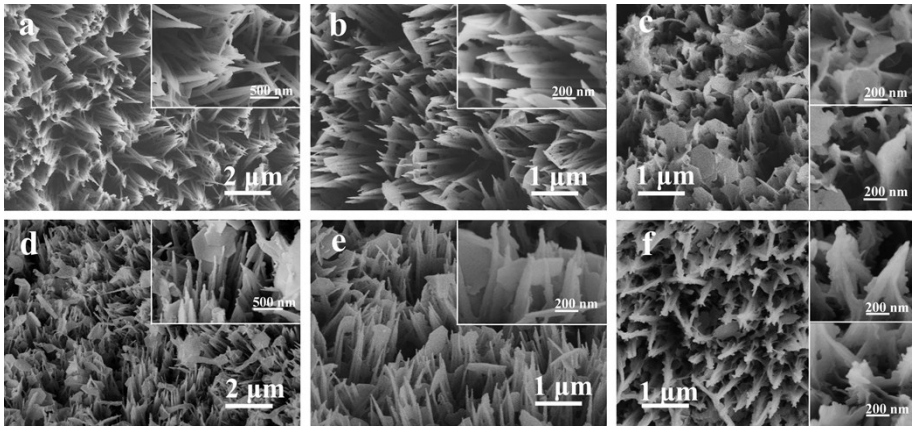

Figure S12 SEM images of dense $Co(CO_3)_{0.5}(OH)\cdot 0.11H_2O$ nanowire array in high-concentration solution at 75°C for 20 min (a), 40 min (b) and 60 min (c) and 100°C for 20 min (d), 40 min (e) and 60 min (f).

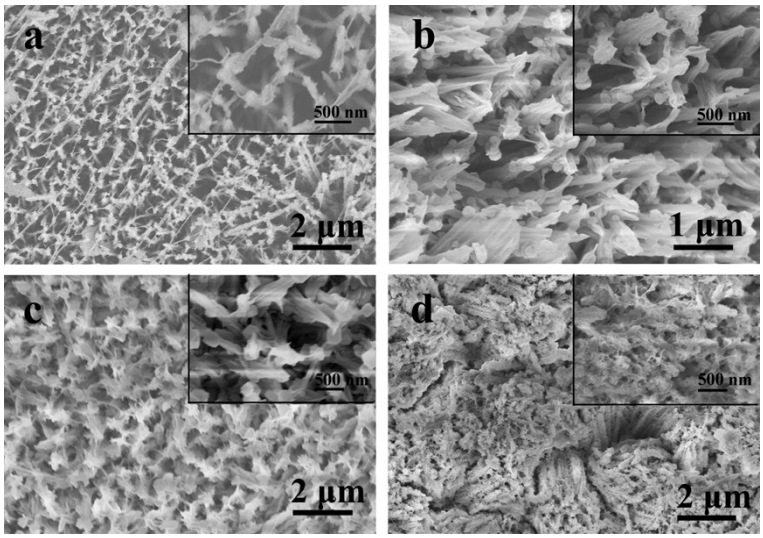

Figure S13 SEM images of less-dense $Co(CO_3)_{0.5}(OH)\cdot 0.11H_2O$ nanowire array in high-concentration solution at 75°C for 15 min (a), 30 min (b) and 60 min (c, d) if gently shaking reaction vessel during the transformation. Some metastable flocs were generated around nanowires which would give rise to ZIF-67 crystals. These morphologies were not reproducible.

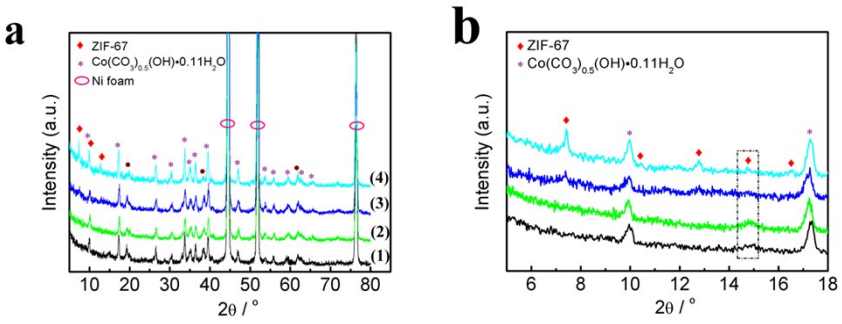

Figure S14 XRD patterns of less-dense $Co(CO_3)_{0.5}(OH)\cdot 0.11H_2O$ nanowire array at the range of 5°~80° (a) and 5°~18° (b) in low-concentration solution at 75°C for different reaction time: 60 min (1), 120 min (2), 180 min (3), 240 min (4). Some unidentified peaks emerged in XRD patterns (a), and it could be seen in (b) that prolonging the reaction time resulted in more ZIF-67 crystals, indicating that the crystallization of ZIF-67 continuously proceeded with the consumption of metastable phase formed at the initial stage, it was a time-dependent process.

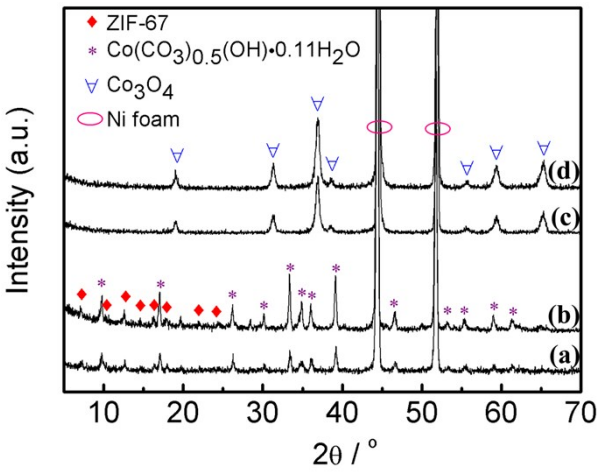

Figure S15 XRD patterns of ZIF-CSNWA (a), ZIF-NTA (b), Co_3O_4-CSNWA (c) and Co_3O_4-NTA (d).

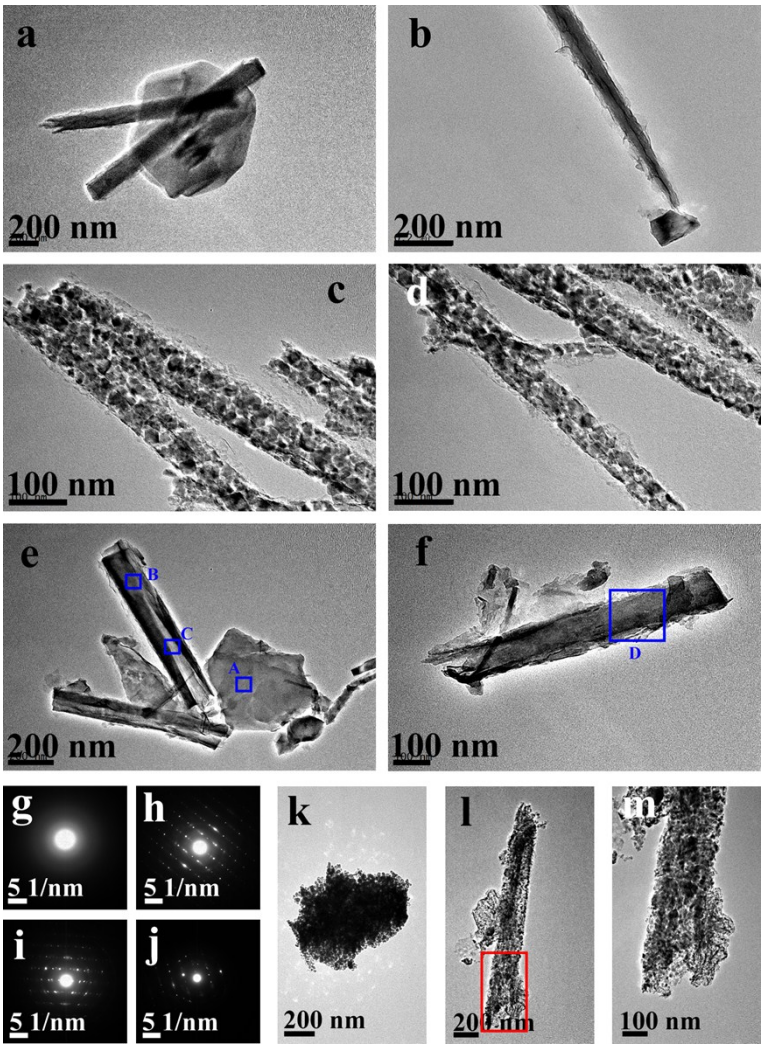

Figure S16 TEM images of ZIF-CSNWA (a, b), Co_3O_4-CSNWA (c, d) and ZIF-NTA (e, f); the corresponding electron diffraction patterns of g, h, I and j corresponds to the rectangular area A, B and C in (e) and area D in (f); TEM images of ZIF-67-derived Co_3O_4 particle (k), Co_3O_4-NTA (l, m). (m) showed the enlarged image of the red rectangular area in (l). It was found out that there was still residual $Co(CO_3)_{0.5}(OH)\cdot 0.11H_2O$ inside the obtained nanotubes here, they composed of $Co(CO_3)_{0.5}(OH)\cdot 0.11H_2O$ and ZIF-67 phases (h-j); the resulting Co_3O_4 nanotube was mesoporous and had 10 ~ 20 nm of particle size (m), which was much smaller than that of directly converted Co_3O_4 from $Co(CO_3)_{0.5}(OH)\cdot 0.11H_2O$ (40 ~ 50 nm, in c, d).

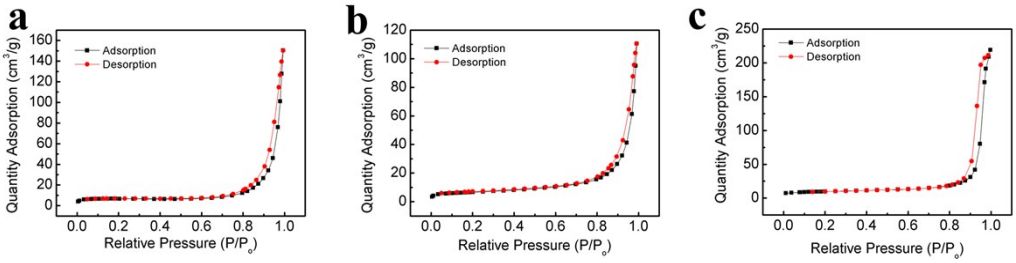

Figure S17 Nitrogen adsorption–desorption isotherms of Co_3O_4-NWA (a), Co_3O_4-CSNWA (b) and Co_3O_4-NTA (c)

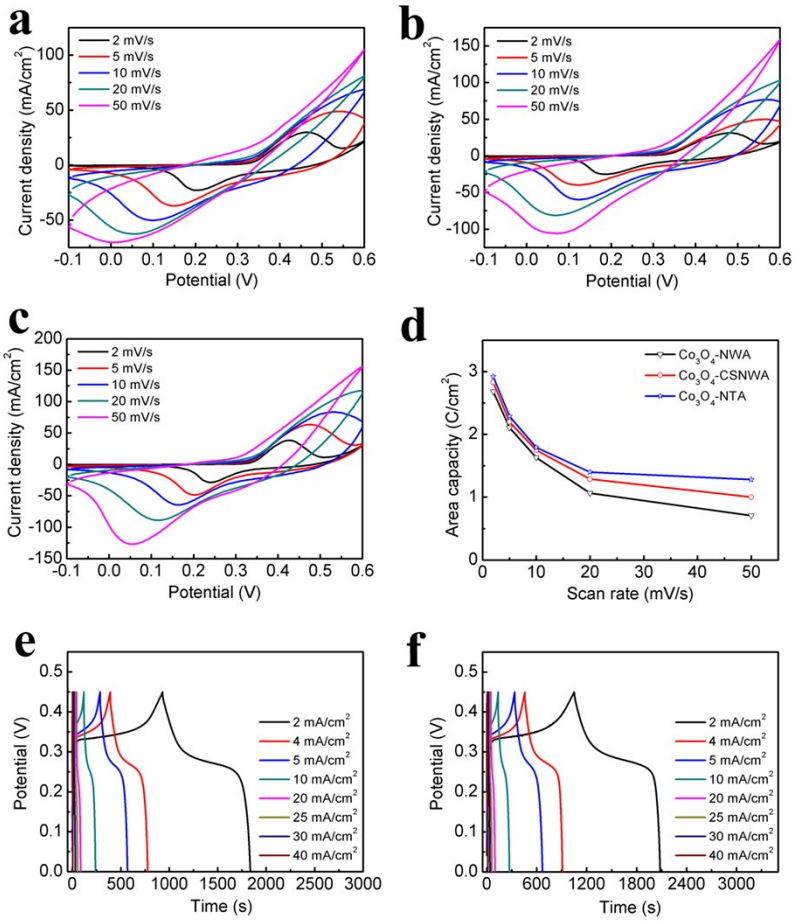

Figure S18 CV plots of Co_3O_4-NWA (a), Co_3O_4-CSNWA (b) and Co_3O_4-NTA (c) at the scan rate of 2, 5, 10 and 20 mV/s; the calculated area capacity values of Co_3O_4-NWA, Co_3O_4-CSNWA and Co_3O_4-NTA from CV plots (d); galvanostatic charge-discharge curves of Co_3O_4-NWA (e) and Co_3O_4-CSNWA (f) at the current density of 2, 4, 5, 10, 20, 25, 30 and 40 mA/cm^2.

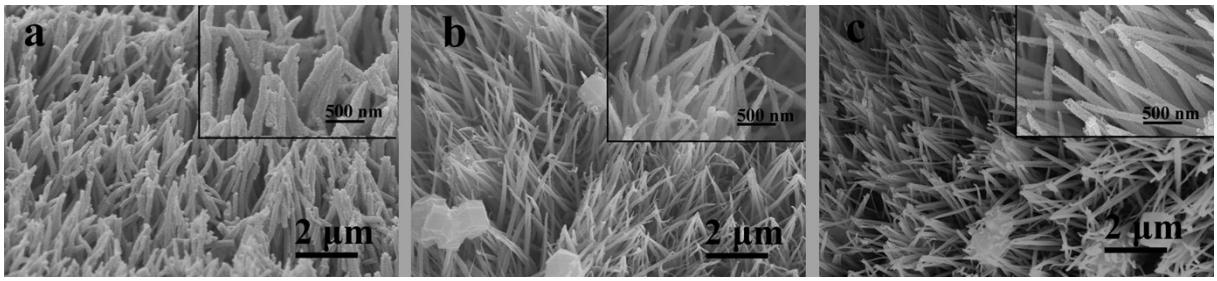

Figure S19 The resulting SEM images of Co_3O_4-NWA (a), Co_3O_4-CSNWA (b) and Co_3O_4-NTA (c) at the current density of 20 mA/cm^2 after 5000 cycles.